0273-2289/00/89/0015/$14.00

Bioconversion of Cellulose into Ethanol by Nonisothermal Simultaneous Saccharification and Fermentation

KYEONG-KEUN OH,[1] SEUNG-WOOK KIM,[2] YONG-SEOB JEONG,[3] AND SUK-IN HONG*,[2]

[1]Department of Industrial Chemistry, Dankook University, Cheonan 330-714, Korea; [2]Department of Chemical Engineering, Korea University, Seoul 136-701, Korea, E-mail: sihong@kuccnx.korea.ac.kr; and [3]Department of Food Science and Technology, Chonbuk National University, Chonju 560-756, Korea

Received September 1, 1999; Revised February 1, 2000; Accepted February 1, 2000

Abstract

The kinetic characteristics of cellulase and β-glucosidase during hydrolysis were determined. The kinetic parameters were found to reproduce experimental data satisfactorily and could be used in a simultaneous saccharification and fermentation (SSF) system by coupling with a fermentation model. The effects of temperature on yeast growth and ethanol production were investigated in batch cultures. In the range of 35–45°C, using a mathematical model and a computer simulation package, the kinetic parameters at each temperature were estimated. The appropriate forms of the model equation for the SSF considering the effects of temperature were developed, and the temperature profile for maximizing the ethanol production was also obtained. Briefly, the optimum temperature profile began at a low temperature of 35°C, which allows the propagation of cells. Up to 10 h, the operating temperature increased rapidly to 39°C, and then decreased slowly to 36°C. In this nonisothermal SSF system with the above temperature profile, a maximum ethanol production of 14.87 g/L was obtained.

Index Entries: Kinetic modeling; temperature profile; nonisothermal simultaneous saccharification and fermentation.

Introduction

With the increasing shortage of petroleum reserves, cellulosic materials have been recognized as one of the most promising alternatives to supply

*Author to whom all correspondence and reprint requests should be addressed.

our chemical and energy needs. The ethanol produced from cellulosic biomass has many advantages over traditional petroleum fuels, such as the diversification in the supply of transportation fuels, the prevention of air pollution, and the decrease in the rate of carbon dioxide production *(1,2)*. Ethanol from cellulosic biomass is produced in a two-step process. First, the cellulose is enzymatically hydrolyzed into glucose, and then the glucose is fermented to produce ethanol. Enzymatic hydrolysis of cellulose is known to have many advantages over acidic hydrolysis, but the rate of enzymatic hydrolysis is considerably slower than that of acidic hydrolysis. Cellobiose and glucose are known to inhibit the activities of cellulase enzymes even at low concentrations *(3)*. In the separate hydrolysis and fermentation and the simultaneous saccharification and fermentation (SSF) processes, the enzyme is the most significant cost factor, and therefore, enzyme loading must be kept at the lowest possible level. SSF is carried out under a sugar-limited condition, thereby reducing the inhibition effect on the enzyme. Although ethanol and other fermentation products can also inhibit enzymatic activity, the inhibition is considered to be much weaker than that caused by glucose and cellobiose. Through SSF, one can minimize product inhibition and simultaneously increase the conversion of cellulose to ethanol. Many researchers have extensively studied SSF to achieve low enzyme loading, a faster rate of hydrolysis, and high production yields *(4–8)*. However, the main difficulty associated with the SSF process is the difference in the optimum temperatures between the hydrolysis and the fermentation processes. The optimum temperature for ethanol fermentation is almost 30°C, whereas the optimum for enzymatic hydrolysis is nearly 50°C. Typically, the SSF process is operated at or near 38°C in order to retain the viability of microorganisms. However, at this temperature, the cellulase enzyme cannot achieve its fullest potential as a catalyst. Thus, the compromised temperatures must be used in the SSF process to produce the ethanol effectively. For this reason, the effects of temperature on the saccharification of cellulose and the fermentation of glucose should be investigated.

The objectives of this study were to develop a set of equations that account for the temperature effect, to find the optimum temperature profile for maximizing the production of ethanol in SSF by using the numerical parameters obtained, and to test the validity of the approach by comparing the predicted values with typical experimental results.

Mathematical Model

Table 1 summarizes the rate expressions used in this study. Mathematical models have been developed for the hydrolysis of cellulose *(9)* and expressed for ethanol fermentation by a Monod-type relationship *(10)*. The cellulose–cellulase system is composed of two reaction phases. The hydrolysis of cellulose is a heterogeneous reaction occurring at the solid–liquid interface of the biomass particles. By contrast, the subsequent breakdown of cellobiose to glucose is catalyzed in the liquid phase by β-glucosidase. The model equations include noncompetitive inhibition of

Table 1
Rate Equations
for Saccharification and Ethanol Fermentation

$$r_1 = -\frac{k_1' C e^{(-\lambda_1 t)}}{1 + \frac{B}{K_{1B}} + \frac{G}{K_{1G}}} \quad (1)$$

$$r_2 = -1.056(r_1) - \frac{k_2' B e^{(-\lambda_2 t)}}{K_m\left(1 + \frac{G}{K_{2G}}\right) + B} \quad (2)$$

$$r_3 = -1.053[1.056(r_1) + (r_2)] \quad (3)$$

$$\frac{dX}{dt} = \mu_m \frac{G}{G + K_G} X\left(1 - \frac{P}{P_m}\right)^a \quad (4)$$

$$\frac{dP}{dt} = m_m\left(\frac{G}{G + K_P}\right)\left(1 - \frac{P}{P_m'}\right)^\beta X \quad (5)$$

cellulase by cellobiose and glucose, noncompetitive inhibition of β-glucosidase by glucose, and substrate inhibition by cellobiose. Enzyme deactivation was considered and lignin concentration was assumed negligible, because pure cellulose was used as a substrate. The hydrolysis rate further decreases owing to the transformation of cellulose into a less digestible form. This aspect was included in the above rate expression. The degree of structural transformation can be measured in terms of the relative digestibility of cellulose, which is defined as the ratio between the hydrolysis rate of residual cellulose and the hydrolysis rate of fresh cellulose. During the course of an alcohol fermentation process, ethanol accumulates in the broth to such an extent that the metabolic activity of microorganisms is suppressed. In this study, the various models were tested for batch cultures of yeast. Two kinetic models are proposed to describe the kinetic pattern of ethanol inhibition on the specific rates of growth and ethanol fermentation.

Materials and Methods

Thermocontrolled Bioreactor

Figure 1 depicts the experimental setup used. The reactor is made of Pyrex glass and stainless steel with a total volume of 1.5 L and a working volume of 700 mL. As a typical bioreactor, the condenser is on the reactor and there are two impellers and four baffles in the reactor, for the effective agitation of insoluble substrate. Anaerobic conditions were maintained by sparging N_2 gas into the fermentation broth. After the cells entered the exponential growth phase, the N_2 flow was stopped and the culture was

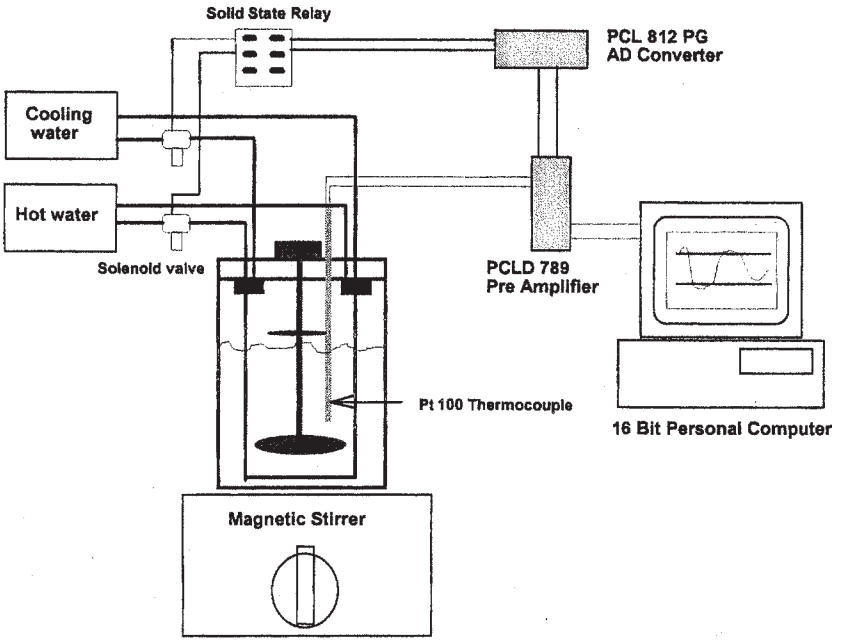

Fig. 1. Schematic diagram of temperature-controlled fermentor system.

kept anaerobic by the CO_2 evolved in the fermentor. The temperature controller consists of a 16-bit personal computer, A/D, D/A converter (PCL-812PG Multi-lab card; Advantech Co); amplifier (PCLD-789 Amplifier/Multiplexer board; Advantech); and solid-state relay (NTH-2003; New Young, Korea). The temperature profile generated by Excel program or mathematical modeling was compared with temperature measured by a thermistor immersed in the fermentation broth. The change in temperature with time was sent to solid-state relay, which controlled the solenoid valve for heating or cooling water. The temperature differences were measured 64 times per second and controlled at ±0.2°C.

Organism and Media

Brettanomyces custersii H_1-55 was derived through genetic improvements of *B. custersii* CBS 5512, a promising glucose and cellobiose fermenting yeast for the SSF of cellulose for ethanol production. It was maintained by transferring to fresh agar slants each month and storing at 4°C. The liquid culture containing 20 g/L of glucose, 10 g/L of yeast extract, and 10 g/L of bacto-peptone was prepared for inoculation. Glucose was sterilized separately from the other components and mixed aseptically.

Enzyme

Cellulase from *Trichoderma reesei* (Celluclast 1.5L) and β-glucosidase (Novozym 188) were purchased from Novo, Denmark. The cellulase and

β-glucosidase have a specific filter paper activity of 33.0 filter paper units (FPU)/mg and 62.2 cellobiose units (CBU)/mg, respectively. They were diluted with sodium citrate buffer (pH 4.8). The resulting enzyme activities of the cellulase and β-glucosidase were measured to be 19 FPU/mL and 20 CBU/mL, respectively.

Substrate

Purified cellulose, α-cellulose, was purchased from Sigma, Germany. The powder of α-cellulose contained long particles 10–20 μm in diameter. The crystallinity of α-cellulose was 80.56% measured by an X-ray diffractometer. The cellulose was mixed with sodium citrate buffer (pH 4.8) before using and agitated for 12 h to allow maximum swelling.

Analytical Methods

Total reducing sugars were measured by the dinitrosalicylic acid method with glucose as the standard. Glucose was measured by the glucose oxidase/peroxidase method *(11)*. Because glucose and cellobiose were the major components of the reducing sugars, the amount of cellobiose was estimated by subtracting glucose from total reducing sugars. Ethanol was analyzed by a gas chromatograph (HP 5890; Hewlett Packard) equipped with a flame ionization detector and HP-1 column. The cell concentration in the batch culture was assayed by measuring the absorbance of a sample at 590 nm with a spectrophotometer (Spectronic 20; Bausch and Lomb). A calibration curve was used to convert the absorbance into dry cell weight per unit volume of the medium.

Determination of Model Parameters and Optimization of Temperature Profile

Determination of the parameters was achieved by performing critical experiments, each one examining the effect of a specific component of the SSF system. The major components of SSF are cellobiose, glucose, and ethanol. Their interaction with the hydrolytic enzymes is expected to have a significant effect on the progress of cellulose hydrolysis and fermentation. The appropriate forms of expressions were regressed to the collected kinetic data using nonlinear regression algorithms to determine the parameters and, at the same time, to examine the predictive ability of the respective model equation. The employed nonlinear regression algorithm was developed based on the Levenberg–Marquardt least squares minimization procedure *(12)*. A mathematical model, accounting for the effects of temperature, that describes the hydrolysis of the cellulose and glucose fermentation process has been developed. Using the optimization routine associated with an integration routine based on the Runge–Kutta method, the optimized temperature profile for maximizing the ethanol production was determined.

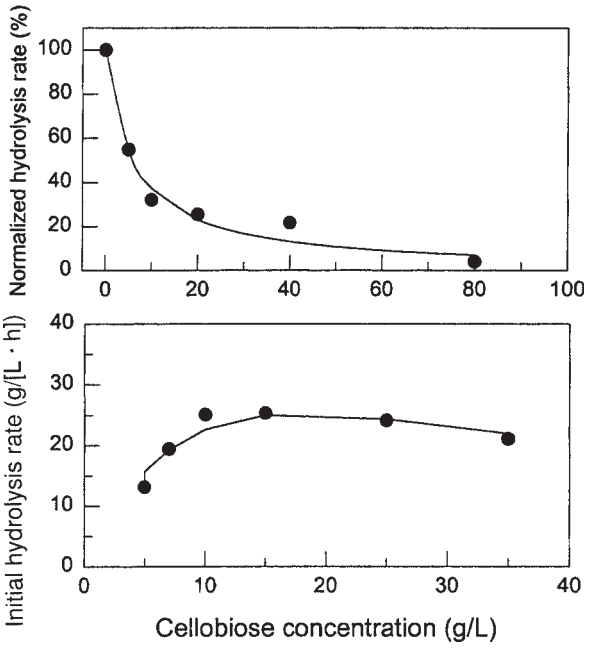

Fig. 2. Dependencies of the cellulase and β-glucosidase activity on cellobiose concentration with cellulase activity of 30 FPU/g-cellulose and β-glucosidase activity of 40 CBU.

Results and Discussion

Characterization of Enzyme Kinetics

Cellobiose is the direct product of cellulase action, and it has a strong inhibitory impact on the activity of the enzyme. The effect of cellobiose on cellulase activity was examined in the concentration range of 0–80 g/L. As shown in Fig. 2, at a cellobiose concentration of 10 g/L, the initial hydrolysis rate of cellulase was reduced by 70%. At concentrations >60 g/L, the cellulase lost approx 90% of its activity. When the cellobiose inhibition assay was extrapolated to time zero, the initial cellobiose concentration was the only variable in Eq. 1 (*see* Table 1), and we could get the K_{1B} of 6.0446 g/L. Cellobiose serves as the substrate for β-glucosidase. The kinetics of cellobiose hydrolysis were investigated by varying the substrate concentration in the range from 5 to 35 g/L. For concentrations up to 15 g/L, there was no evidence of substrate inhibition on β-glucosidase activity, and the kinetics follow the Michaelis–Menten equation. Because the cellobiose concentration cannot be more than 10 g/L in the typical SSF process, the substrate inhibition by cellobiose was not considered. After simplifying Eq. 2 by extrapolation to time zero, we could get the Michaelis–Menten constant K_m of 9.2856 g/L.

Figure 3 describes the effect of glucose concentration on the cellulase and β-glucosidase activity in the range of glucose concentrations from 0 to

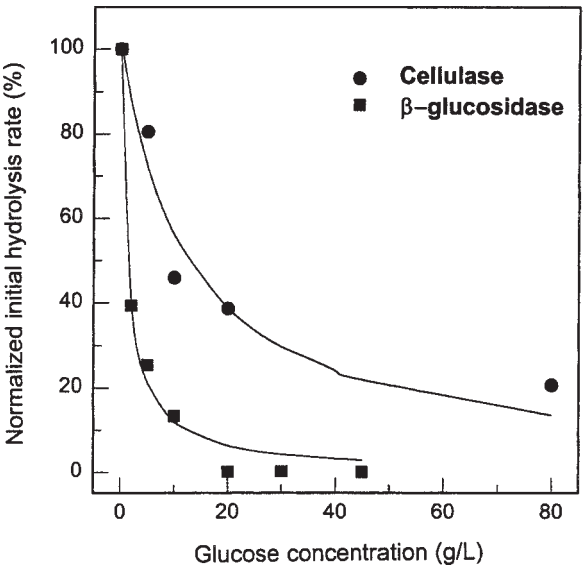

Fig. 3. Dependencies of the activities of cellulase and β-glucosidase on the glucose concentration in the presence of 89 g/L of α-cellulose and 10 g/L of cellobiose, respectively.

Table 2
Kinetic Parameters of Cellulase and β-Glucosidase
Regarding Their Interactions with Products

Parameter	Parameter value	Enzyme/inhibitor
k_1'	0.1530 (h)	Cellulase
k_2'	52.4360 (g/[L·h])	β-Glucosidase
K_{1B}	6.0446 (g/L)	Cellulase/cellobiose
K_{1G}	12.3837 (g/L)	Cellulase/glucose
K_{2G}	0.3270 (g/L)	β-Glucosidase/glucose
K_m	9.2856 (g/L)	β-Glucosidase
λ_1	0.0232 (h)	Cellulase
λ_2	0.0144 (h)	β-Glucosidase

80 g/L. The initial hydrolysis rate of cellulose by glucose was decreased to <20% at a glucose concentration of 5 g/L and about 60% at a glucose concentration of 20 g/L. Equation 1 can satisfactorily predict the rate of cellulose hydrolysis over a wide range of glucose concentrations. The nonlinear regression algorithm yielded a K_{1G} of 12.3837 g/L. For β-glucosidase, at a glucose level of only 5 g/L, 80% of the β-glucosidase activity was lost. At a glucose concentration of 20 g/L, β-glucosidase was practically inactive. The low value of the inhibition constant, K_{2G}, of 0.327 g/L, determined by nonlinear regression of Eq. 2, shows that β-glucosidase is extremely sensitive to glucose. Table 2 provides a summary and overview of the interaction of the enzymes with cellobiose and glucose. Cellulase and β-glu-

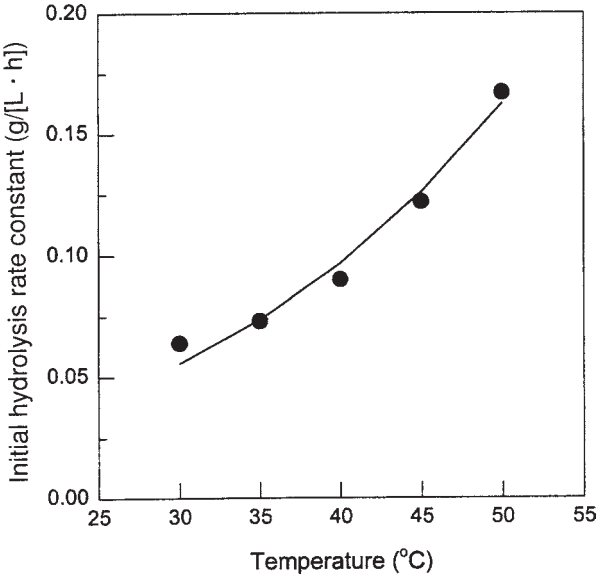

Fig. 4. Dependency of the initial hydrolysis rate constant of cellulase on the temperature with the cellulase activity of 30 FPU/g-cellulose.

cosidase exhibit diverse kinetic behaviors and are affected to a considerably different extent by the presence of cellobiose and glucose.

Effects of Temperature on Hydrolysis of Cellulose

Dependence of Initial Hydrolysis Rate

To exclude the effect of product inhibition, the initial hydrolysis rates were measured at different temperatures from 30 to 50°C. Figure 4 shows the effect of temperature on the hydrolysis rate. At 30°C, the initial hydrolysis rate was 0.064 g/(L·h). However, the initial hydrolysis rate at 50°C was 0.167 g/(L·h). As the temperature increased, the production of the reducing sugar and the dependence of hydrolysis rate on temperature increased; that is, in the temperature range of 35–40°C, the rate of increase in initial hydrolysis per unit degree was 4.6%/°C, but that in the range of 40–45°C was 7.1%/°C. The effect of temperature on the specific hydrolysis rate is quantitatively described by the following Arrhenius equation:

$$k_i(T_1) = k_i(T_2)\exp[-\Delta H^{\#}/R(1/T_1 - 1/T_2)]$$

in which $k_i(T_1)$ and $k_i(T_2)$ are the rate constant at the absolute temperature T_1 and T_2; R is the gas constant (=8.314 × 10^{-3} kJ/[mol·K]); and $-\Delta H^{\#}$ is the activation enthalpy of the reaction described by rate coefficient k_i(kJ/[mol·K]). We obtained $-\Delta H^{\#}$ of 43.6483 (kJ/[mol·K]).

Dependence of Deactivation Rate of Enzyme

As temperature increases, the production of glucose and the dependence on the hydrolysis rate increase. However, the thermal deactivation

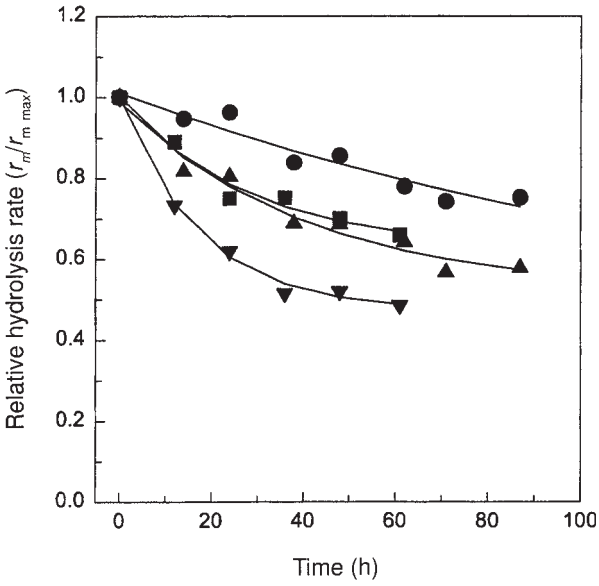

Fig. 5. Comparison of relative hydrolysis rates of cellulose at various temperatures: (●) 33°C; (■) 38°C; (▲) 43°C; and (▼) 48°C.

of the enzyme will be severe at high temperatures. Figure 5 shows the comparison of relative activities of cellulase to temperature variation. The dependence of enzyme activity on temperature was measured by the incubated cellulase samples at various temperatures for different periods of time. Decay of filter paper activity at constant temperature was fitted to a first-order deactivation model: $r_m / r_m^{max} = \exp(-\lambda t)$. At 33°C, relatively slight deactivation of the enzyme was observed. However, relative activity decreased dramatically at 48°C, and after 60 h, the relative activity of cellulase was lower than all other values obtained at lower temperatures.

Effects of Temperature on Fermentation of Glucose

Estimation of the effect of temperature on the kinetic parameters in batch culture requires the use of a mathematical model for ethanol fermentation. In the present analysis, the various models were tested for batch cultures of *B. custersii* H_1-55. As a result, the model that was reported by Levenspiel *(13)* in 1980 was used for estimation of the kinetic parameters at various temperatures (*see* Eqs. 4 and 5 in Table 1). The effect of temperature change on cell growth and ethanol production was investigated in the temperature range of 35–45°C (Fig. 6). This range is applicable to the limited reaction temperature in the SSF process. At 35°C, the maximum specific growth rate was as high as 0.56/h, but as the temperature increased, the maximum specific growth rate decreased. At 45°C, the maximum specific growth rate was 0.15/h.

The change in surrounding temperature can have a direct influence on the reaction rate of cells, characteristics of metabolism, and structure of

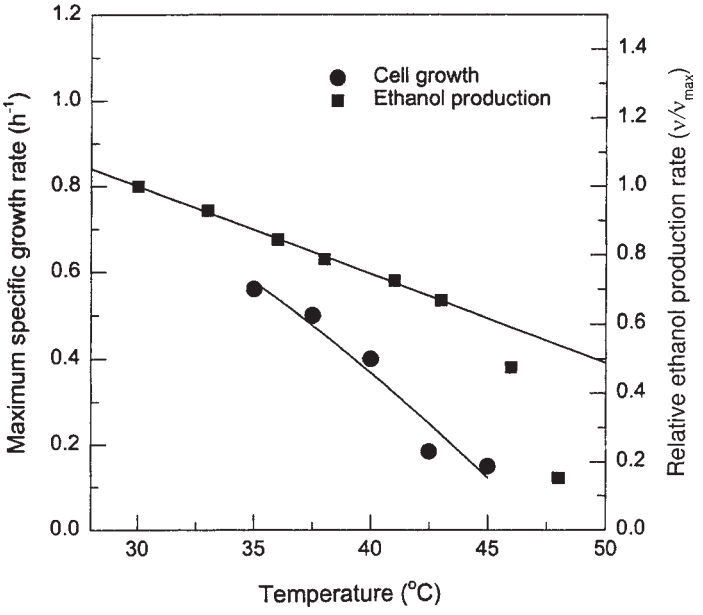

Fig. 6. Temperature dependencies of maximum growth rate and relative ethanol production rate of H_1-55 strain with YPD medium.

cells. The mechanism of metabolic control, enzyme reaction, and cell permeation can also be affected. Accordingly, the dependence of temperature is an unavoidable parameter for ethanol fermentation.

As shown in Fig. 6, in the range of 30–42.5°C, the maximum specific production rate decreased by 2.5% with a 1°C increase in temperature. Above 42.5°C, the rate of ethanol production decreased rapidly.

Monod Saturation Constant K_G *and* K_P

Figure 7 illustrates the dependences of K_G and K_P in Eqs. 3 and 4. At 35°C, K_G, the Monod saturation constant for cell growth, was 2.483 g/L, and at 45°C, K_G was 4.1 g/L. The K_G constant increased linearly by 0.167 g/L in this temperature range. By comparison, the Monod saturation constant for ethanol production, K_P, was much more sensitive to the temperature than K_G. The dependence of K_P on temperature increased with an increase in temperature. At 35°C, K_P was as low as 0.51 g/L, but K_P was as high as 5.57 g/L at 45°C.

Effect of Ethanol Concentration

The primary limiting factor in ethanol production is the effect of ethanol on yeast growth and fermentation. In general, as the initial amount of ethanol in the medium is increased, the specific growth rate and specific ethanol production rate decrease. Tolerance to high concentrations of ethanol is strain dependent with a maximum allowable concentration of about 10% (w/v) for growth and 20% for ethanol production being exhibited in the most tolerant strains *(14)*. Figure 8 shows the effect of ethanol on growth

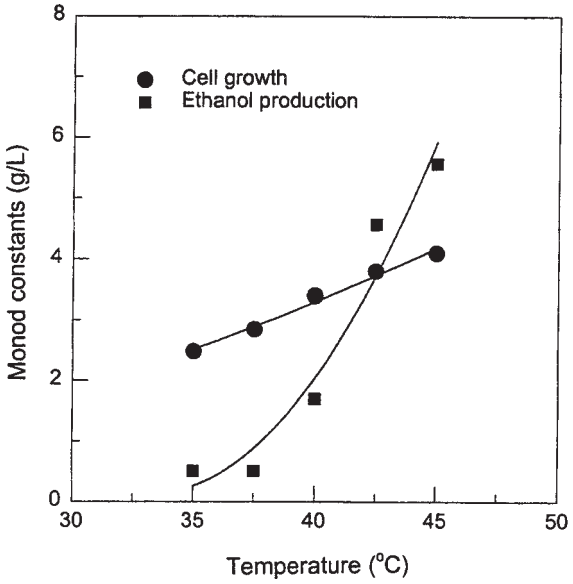

Fig. 7. Temperature dependencies of Monod saturation constant for cell growth and ethanol production with YPD medium.

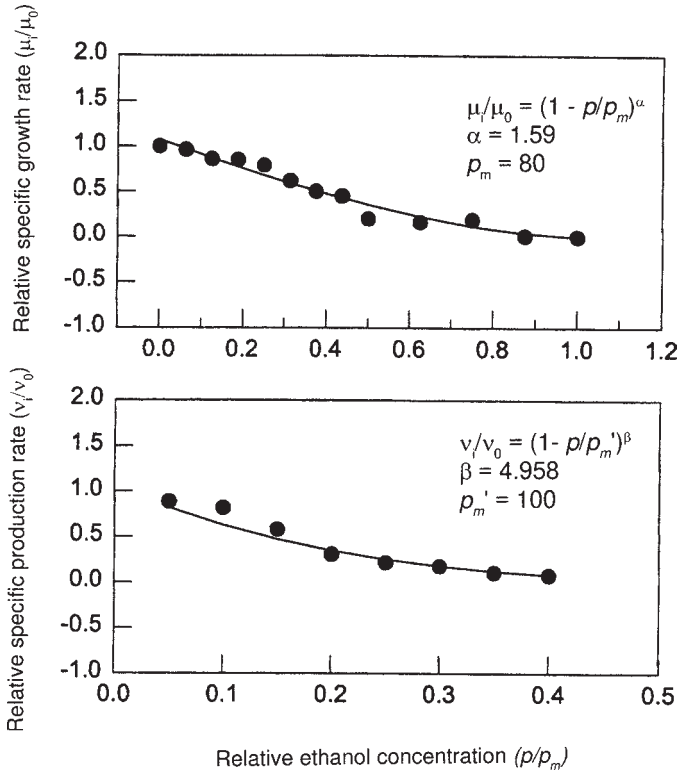

Fig. 8. Inhibitory effects of ethanol concentration on cell growth and ethanol production.

Table 3
Kinetic Parameters of *B. custersii* (H_1-55) at Different Temperatures

Kinetic parameter	35°C	37.5°C	40°C	42.5°C	45°C
Maximum growth rate (h)	0.56	0.50	0.40	0.18	0.15
Relative production rate	0.84	0.79	0.67	0.48	0.15
Monod saturation constant for growth (g/L)	2.48	2.85	3.40	3.83	4.10
Monod saturation constant for production (g/L)	0.51	0.51	1.70	4.57	5.57
Biomass yield (g/g)	0.12	0.14	0.15	0.15	0.12
Ethanol yield (g/g)	0.44	0.44	0.45	0.45	0.43

rate and fermentation rate during batch culture with different initial alcohol concentrations. The plots between μ_i/μ_0 and P/P_m, and ν_i/ν_0 and P/P_m', were well represented by the model proposed by Levenspiel *(13)* to predict the effect of ethanol inhibition on growth and fermentation. The best-fit values of α and β were determined to be 1.59 and 4.95, respectively. The maximum allowable ethanol concentration above which cells do not grow was determined to be 80 g/L, and the ethanol level above which cells stop producing ethanol was 100 g/L. The inhibitory effect of ethanol for production of ethanol was more severe than that for cell growth. To examine the dependence of temperature on the ethanol inhibitory effect, ethanol production was investigated in the temperature range of 33–48°C. In this temperature range, the dependencies of temperature showed a similar tendency.

Kinetic Modeling for Ethanol Fermentation

Table 3 summarizes the parameters derived through critical experiments. In SSF, the glucose concentration can be maintained at a low level, because the glucose produced can be converted into ethanol rapidly. Thus, enzyme inhibition by glucose was not considered. The constant m, which relates to the nongrowth-associated production term of Eq. 5, was negligibly small (below 0.002) *(13)*. We could not obtain the constant m included in Eq. 5 by the experiment; therefore, the m value of 0.211/h from Philippidis et al. *(9)* was substituted in the model. The ethanol yield, $Y_{P/S}$, appeared to be unaffected by temperature over the range 33–48°C, and the value was consistent from 0.43 to 0.45. The kinetic experiments were conducted over the range of initial glucose concentrations of 7–43 g/L, at the various temperatures. Figures 9 and 10 describe the results of the model and experiments at the glucose concentration of 7–12 g/L (data for glucose concentration >25 g/L are not shown). Using the parameter values given in Table 3, good agreement was found between the model and the experimental data. At a glucose concentration >25 g/L, the parameter values from the model were overestimated, compared with those obtained from the experiment. However, because the glucose concentration always is maintained at a low

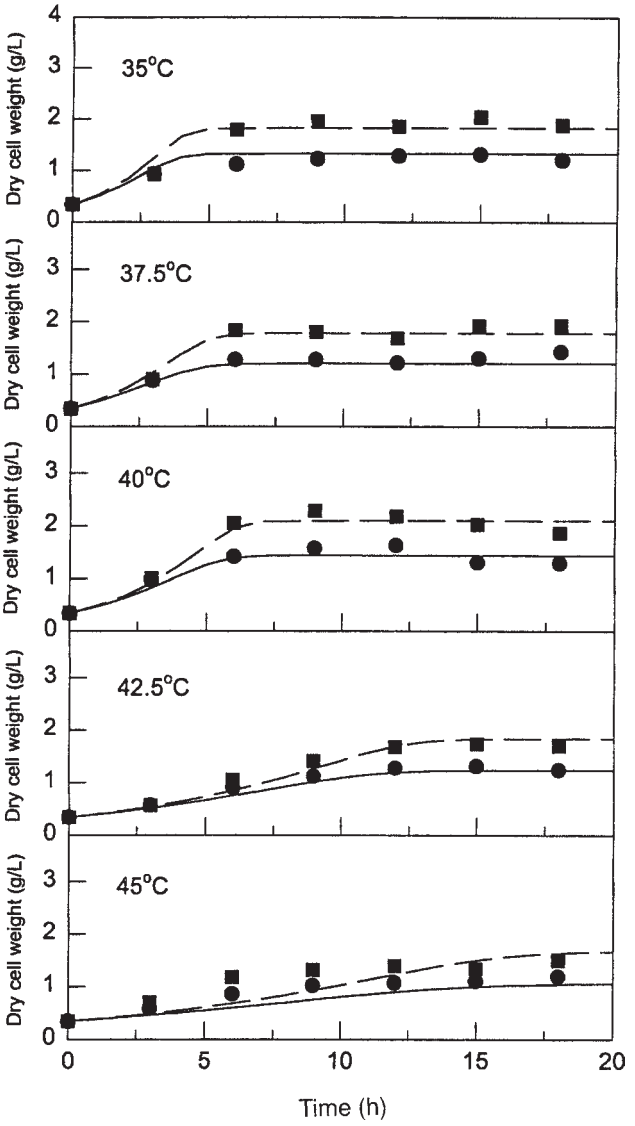

Fig. 9. Experimental data and model simulations for cell growth at various temperatures with glucose concentrations of (●) 7 and (■) 11 g/L.

level in SSF, it was concluded that the models and parameters estimated in this study can be applied to the SSF process.

Optimization of Temperature for Maximizing Ethanol Production

Table 4 summarizes the parameters including the temperature effect. The parameters established the validity over the some range of temperatures. The appropriate forms of model equations including the effects of temperature have been developed. The temperature profile for maximizing the production of ethanol in the nonisothermal SSF was found by using

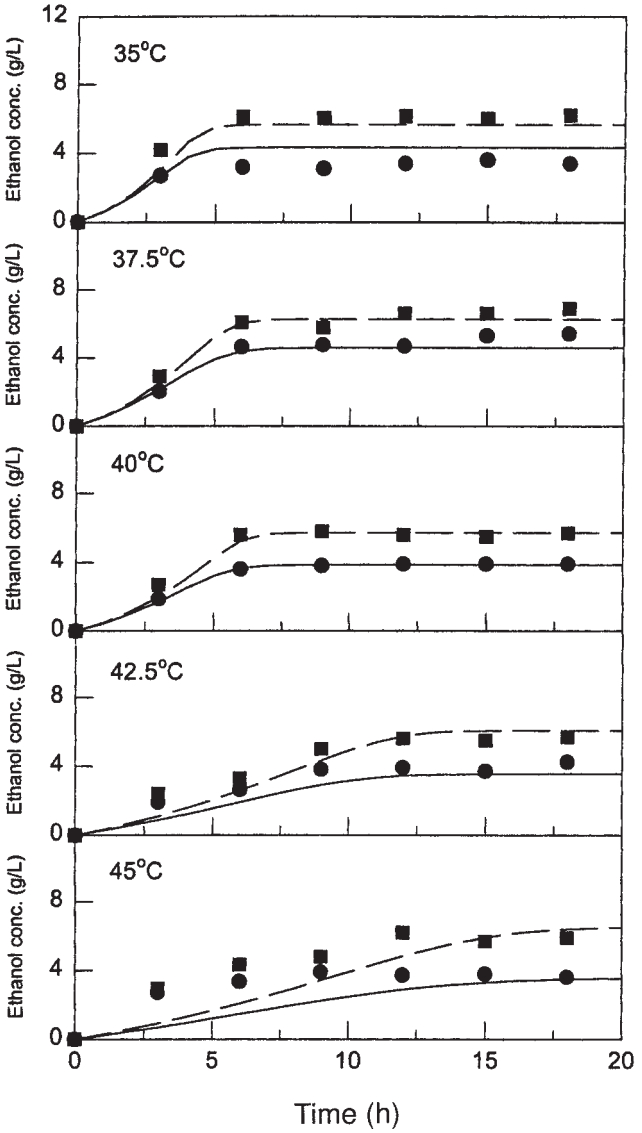

Fig. 10. Experimental data and model simulations for ethanol production at various temperatures with glucose concentrations of (●) 7 and (■) 11 g/L.

the optimization routine (MINOS) associated with an integration based on the Runge–Kutta method *(15)*. Figure 11 shows the optimized temperature profile and ethanol production with α-cellulose at 38 and 42°C, respectively. The operating temperature of SSF was restricted by the temperature tolerance of the microorganisms used. Thus, the upper and lower limits of operating temperature are 30 and 45°C, respectively. Temperature profiling begins with a low level of temperature at 35°C, which allows the propagation of cells during the first 4 h. Up to 7 h, the operating temperature

Table 4
Evaluation of Kinetic Parameters
as a Function of Temperature (35–45°C)

Parameter	Function
k_1'	$0.1626 \exp\left[-43.648\left(\frac{1}{T}-\frac{1}{323}\right)\right]$
k_2'	$52.436 \exp\left[-51.269\left(\frac{1}{T}-\frac{1}{323}\right)\right]$
λ_1	$0.0232 \times (0.0528 \times T - 15.101)$
λ_2	$0.0144 \times (0.0701 \times T - 20.914)$
μ_m	$-7.34 \times 10^{-4} \times T^2 + 0.414 \times T - 57.3006$
m	$-0.025 \times T + 8.75$
K_G	$0.167 \times T - 49.095$
K_P	$0.0421 \times T^2 - 25.761 \times T + 3944.809$

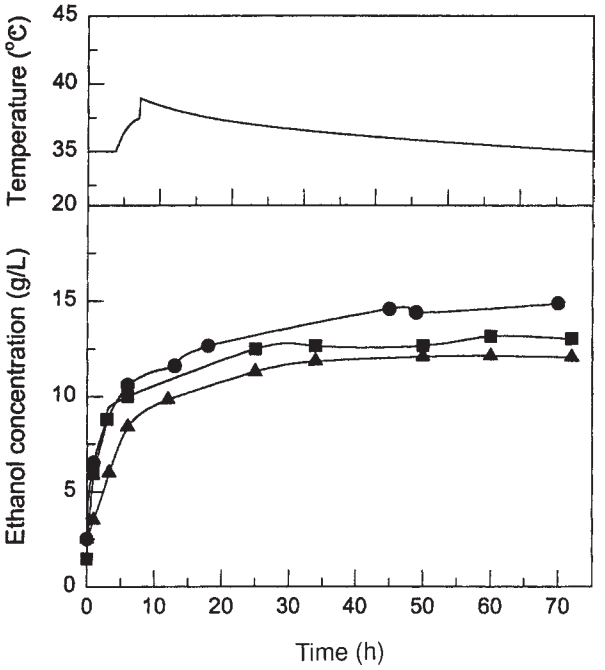

Fig. 11. Optimized temperature profile and ethanol production by SSF with α-cellulose at (■) 38°C, (▲) 43°C, and (●) optimized temperature profile.

increased rapidly up to 38.97°C, after which it decreased slowly to 35.13°C at 72 h. The predicted final concentration of ethanol was 16.17 g/L, and the maximum ethanol concentration of 14.87 g/L was obtained in this nonisothermal SSF, which is 14–21% higher than that of the conventional isothermal SSF.

Nomenclature

k_1' = Specific rate of hydrolysis (h)
k_2' = Lumped constants (g[L·h])
K_m = Michaelis constant of β-glucosidase (g/L)
K_P = Monod saturation constant for ethanol production (g/L)
K_G = Monod saturation constant for cell growth (g/L)
K_{1B} = Inhibition constant of cellulase for cellobiose (g/L)
K_{1G} = Inhibition constant of cellulase for glucose (g/L)
K_{2B} = Inhibition constants of β-glucosidase for cellobiose (g/L)
m = Maintenance energy coefficient (h)
P = Ethanol concentration (g/L)
P_m = Ethanol concentration above which cells do not grow (g/L)
P_m' = Ethanol concentration above which cells do not produce (g/L)
r_1 = Volumetric rate of cellulose utilization (g[L·h])
r_2 = Volumetric rate of cellobiose utilization (g[L·h])
r_3 = Volumetric rate of cellobiose utilization (g[L·h])
X = Cell concentration (g/L)
λ = Specific rate of enzyme deactivation (h)
λ_1 = Specific deactivation rate of cellulase (h)
λ_2 = Specific deactivation rate of β-glucosidase (h)
μ_m = Maximum specific growth rate (h)
μ_i = Specific growth rate of cells in the presence of ethanol (h)
μ_0 = Maximum growth rate of cells in the absence of concentration (h)
ν_i = Specific rate of ethanol production in the presence of ethanol (h)
ν_0 = Maximum rate of ethanol production in the absence of ethanol (h)

References

1. Wyman, C. E. (1994), *Appl. Biochem. Biotechnol.* **45,** 897–915.
2. Himan, N. D., Schell, D. J., Riley, C. J., Bergeron, P. W., and Walter, P. J. (1992), *Appl. Biochem. Biotechnol.* **34/35,** 639–649.
3. Spindler, D. D., Wyman, C. E., and Grohaman, K. (1991), *Appl. Biochem. Biotechnol.* **28/29,** 773–786.
4. Philippidis, G. P. and Smith, T. K. (1995), *Appl. Biochem. Biotechnol.* **51,** 117–124.
5. Kim, J. S., Oh, K. K., Kim, S. W., Jeong, Y. S., and Hong, S. I. (1999), *J. Microbiol. Biotechnol.* **9(3),** 297–302.
6. Asenjo, J. A., Sun, W. H., and Spencer, J. L. (1991), *Biotechnol. Bioeng.* **37,** 1087–1094.
7. Huang, S. Y. and Chen, J. C. (1988), *J. Ferment. Technol.* **66,** 509–516.
8. Barron, N., Marchant, R., McHale, L., and McHale, A. P. (1995), *Appl. Microbiol. Biotechnol.* **43,** 518–520.
9. Philippidis, G. P., Spindler, D. D., and Wyman, C. E. (1992), *Appl. Biochem. Biotechnol.* **34/35,** 543–556.
10. Pirt, S. J. (1975), *Principles of Microbe and Cell Cultivation*, 1st ed., John Wiley & Sons, New York.
11. Ghose, T. K. (1988), *Pure Appl. Chem.* **59(2),** 257–268.
12. Marquardt, D. W. (1963), *J. Soc. Ind. Appl. Math.* **11,** 431–441.
13. Levenspiel, O. (1980), *Biotechnol. Bioeng.* **22,** 1671–1687.
14. Bailey, J. E. and Ollis, D. F. (1986), *Biochemical Engineering Fundamentals*, 2nd ed., McGraw-Hill, New York.
15. Bruce, A. M. and Michale, A. S. (1987), *MINOS 5.1 user's guide*. Stanford University, CA.